# We are IntechOpen, the world's leading publisher of Open Access books Built by scientists, for scientists

**4,800**
Open access books available

**122,000**
International authors and editors

**135M**
Downloads

Our authors are among the

**154**
Countries delivered to

**TOP 1%**
most cited scientists

**12.2%**
Contributors from top 500 universities


WEB OF SCIENCE™

Selection of our books indexed in the Book Citation Index in Web of Science™ Core Collection (BKCI)

## Interested in publishing with us?
## Contact book.department@intechopen.com

Numbers displayed above are based on latest data collected.
For more information visit www.intechopen.com

# 18

# Regenerated Fibre Bragg Gratings

John Canning[1], Somnath Bandyopadhyay[2], Palas Biswas[2], Mattias Aslund[1], Michael Stevenson[1] and Kevin Cook[1]
[1]*Interdisciplinary Photonics Laboratories (iPL), Madsen Building F09, School of Chemistry, University of Sydney, NSW, 2006*
[2]*Fibre Optics Laboratory, Central Glass and Ceramic Research Institute (CGCRI), Council of Scientific & Industrial Research, Kolkata - 700032,*
[1]*Australia*
[2]*India*

## 1. Introduction

Silica remains the key optoelectronic and photonic medium, the essence of nearly all modern optical transport systems. Engineering of silica in its various forms ranges from 1 to 3-dimensional waveguide and periodic structures, including recent interest in 3-D photonic crystals. Most of the processing methods involve complex vapour deposition and various co-dopants, which have an advantage of overcoming the lack of finesse involved with general formation of glass structure through high temperature processing and quenching. Nevertheless, to obtain micron or sub-micron precision over the processing of glass for device purposes, invariably post processing methods are commonly used, ranging from etching of systems with dopants, often through patterned masks, to laser processing using UV to mid IR lasers. Concrete examples of micron scale laser processing of glass include direct written waveguides, Bragg gratings in waveguides and optical fibres and photonic crystals. The drawback with these post-processing techniques is that they often produce glass that is structurally less stable than the starting phase. For many applications the thermal stability of laser induced glass changes determines the limits in which they can operate – an excellent example which will form the basis for this chapter, is the optical fibre Bragg grating.

Fibre Bragg gratings are used in many industrial and technological applications. Within standard telecommunications applications, for example, type I fibre Bragg gratings that can operate to 80˚C for 25 years are required – such gratings can in principle operate for lengthy periods up to 300˚C. Gratings that can operate at temperatures well above standard telecommunication requirements are critical to the success of many real time sensing applications. In the oil and gas industries, an alternative application, although standard oil bores are typically quoted as having an environment no more than ~(180-250)˚C [Schroeder et al. 1999; Kersey 2000], variations can occur and the increasing depth of the next generation bores suggest sensors that can operate to 400˚C or more are desirable for long term or permanent operation. In industries involving high temperature furnaces, such as aluminium smelting or coal based power stations, it would be of interest to be able to monitor temperatures in excess of 1000˚C. Similar temperature requirements span many

Source: Frontiers in Guided Wave Optics and Optoelectronics, Book edited by: Bishnu Pal,
ISBN 978-953-7619-82-4, pp. 674, February 2010, INTECH, Croatia, downloaded from SCIYO.COM

other types of industries: structural health monitoring of buildings need to be able to operate in temperatures above 400˚C in the event of a serious fire [Cardoza et al. 2007], engine turbines in various vehicle formats, particularly aircraft, can reach temperatures well above this, whilst the integration into next generation composite structures [Epaarachchi et al. 2009] in many of these applications often need to be carried out in temperatures above (300-400)˚C. Another particularly important industry is the fibre laser sector [Canning 2006 and refs therein]. Presently, fibre Bragg gratings are spliced onto the ends of the fibre using specially designed matched photosensitive cores. However, some fibre mismatch, along with power tolerance issues within doped glass, remains. One approach to dealing with these and to reduce overall costs, is to write gratings directly into the active medium. Unfortunately, we have recently demonstrated that, in $Yb^{3+}$ -doped fibre lasers at least, the UV induced grating index of a type I grating within the doped fibre can be readily annealed at moderate powers (~13W) [Åslund et al. 2005]. Even using femtosecond produced type II gratings, annealing occurs when the internal fields exceed kW, as within a Q-switched fibre laser [Åslund et al. 2008,2009b]. Until these issues are resolved, gratings will continue to be spliced onto the ends of the gain medium.

Within all these applications, the same stringent fabrication capabilities imposed on telecommunications are also increasingly desirable as sensor system and components become more complex than simple low reflection filters. Numerous distributed components raise the challenging specter of cross-talk between devices. Complex filter properties such as apodisation, chirping, phase shifts and more are increasingly in demand. Therefore, ideally there is a need to produce high temperature gratings that retain the best features of the current workhorse, the type I grating. There is a new type of grating attracting worldwide attention that promises to deliver this: the regenerated fibre Bragg grating. It is essentially formed from the initial type I "seed" grating, precipitating through thermal processing with a structure that is set by the laser written seed. For many other applications requiring similar levels of holographic precision by laser processing, the need for tailored and controlled *ultra stabilised* index change remains equally vital. To demonstrate new developments towards these goals we, however, concentrate in this chapter on the 1-D periodic structure of the optical fibre Bragg grating, noting that the general processes are much more widely applicable.

### 1.1 Historical background

Previous studies have already established that the operable temperature of FBGs can be increased by several means, including tailoring the glass composition [Shen et al. 2007; Butov et al. 2006], pre-processing with seed irradiation [Åslund & Canning 2000; Canning et al. 2001], the formation of type-I*n* (or type II*A*) [Xie et al. 1993; Dong et al. 1996; Groothoff & Canning 2004] gratings and type-II [Archambault et al. 1993; Hill et al. 1995] gratings, including those inscribed using femtosecond IR lasers [Grobnic et al. 2006]. For a general review on photosensitivity and grating types, see [Canning 2008a]. Another variant with superior high temperature stability is the so-called "chemical composition grating (CCG)" [Fokine 2002] where a periodic index modulation can be regenerated after erasure of the UV induced type-I grating written in H-loaded germanosilicate fibre, which happens to contain fluorine, if annealed ~1000˚C. The prediction was a local reduction, or increase, of fluorine in the UV-exposed zones at that high temperature through diffusion of hydrogen fluoride. A subsequent study on annealing of type-I gratings at high temperature, however, has shown

that the presence of fluorine is not necessary for this regeneration of index modulation [Trpkovski et al. 2005]. So-called chemical composition gratings (CCG) are found in Er-doped fiber with other dopants such as Ge, Al and Sn – as the number of possible diffusing materials increased, a number of researchers settled on oxygen diffusion (through OH) leading to stoichiometric changes. Very recently, the general phenomenon of regeneration has been found in simple H-loaded germanosilicate fibre [Zhang & Khariziet 2007]. We soon recognized a more general implication of this result – rather than rely on a diffusive interpretation and subsequent polarisability change as the basis for writing gratings, an alternative approach to engineering the index change based on glass structural transformation arising from relaxation of high internal pressures and high temperature processing was proposed. Whilst much work remains to verify details of this approach, it implicitly did not rely on the fibre glass dopants at all (other than maximizing the seed grating strength) and directly led to the development of regenerated gratings in standard photosensitive fibres with transmission rejection >10%/cm and which can tolerate temperatures as high as 1295°C [Bandyopadhyay et al. 2008; Canning et al. 2008b]. The use of hydrogen was important, but not necessarily essential, to obtain index modulation of useful magnitude for very high temperature operation, since it permitted enhanced localisation of the pressure differences between processed and unprocessed regions. The model proposed in Canning et al. 2008b is independent of this and recent work demonstrates that regeneration can be achieved without hydrogen, although for much lower temperature operation [Linder et al. 2009]. In this chapter, we briefly review the hypothesis and demonstrate thermal processing of UV-induced templates that retain the nano-scale precision of the template whilst stabilising the glass change to unprecedented levels. Specifically, we concentrate on studying the thermal properties of regenerated gratings for ultra high temperature operation and show complex behaviour until properly stabilised. There is a linear growth in grating strength with length. Further, we regenerated two types of complex structures (superposed twin grating and a Moiré grating) to demonstrate that all the properties introduced by the seed grating are retained with nm resolution, suggesting that this method could form an advanced processing method for creating holographic structures that go beyond 1-D filters and which have ultra-high thermal stability.

## 2. Thermal stabilisation of seed index change

Prior to regeneration, the relaxation processes describing normal index change involved with type I grating writing is also characterised by a complex distribution of many relaxations with different timescales and different thermal stabilities. This is characteristic of glass preparation within an amorphous regime. In this section we show quite clearly that there is a distinct regeneration process threshold which suggests, upon regeneration there is an overwhelming preference for fewer relaxation processes. Even below this threshold, thermal stabilisation leads to a single relaxation. We postulate that this reduction is uncharacteristic of an amorphous system and that the glass may very well be transforming into a crystalline polymorph.

### 2.1 Type I gratings

Standard type I fibre Bragg gratings have become ubiquitous in telecommunication and related devices. These are thermally stabilised by annealing to operate over the

telecommunications standards between -25 °C and +80 °C for up to 25 years, as predicted by numerous accelerated aging (annealing) models. Generally speaking experimental results have been consistent with these predictions. For new applications, however, the thermal operation of the fibre Bragg gratings needs to be stabilised to much higher temperatures but for many applications these are *temperatures which are still below that characterised by regeneration*. For example, in the oil, gas and mining industries, including seismic exploration and acoustic detection underground and underwater, the grating is expected to operate to temperatures as high as 400 °C. The options available, within certain limitations, are numerous. They include type 1*n* (type IIa) and type I*p* (type Ia) gratings that can operate between 500-800 °C depending on preparation [Canning 2008a and refs therein]; type II damage gratings [Canning 2008] produced by irradiation above the damage threshold of the glass using UV lasers or multiphoton excitation with longer wavelengths and more recent regenerated gratings that are based on glass structural change achieved using type I seed gratings as a template [Bandyopadhyay et al. 2008; Canning et al. 2008b]. The problem with these various methods is that the gratings produced often compromise the ideal properties offered by type I gratings. For example, type I*n* (and type I*p*) require overly long fluencies that often result in not only weaker gratings but a degradation in profile. Thermally more stable type II gratings are associated with large diffractive losses that make them poor choices for distributed systems and given the role of severe structural change, often on the nanoscale, the long term performance remains poorly understood. Regenerated gratings, on the other hand, operate at the highest temperatures ever achieved (up to 1295 °C) and have losses comparable to type I gratings. Unlike any other high temperature gratings, they can also preserve the complex functionality (shown later) of an advanced type I grating making them appear to be the ideal choice. Unfortunately, the local refractive index change is an order of magnitude less than the original type I seed grating making strong gratings with complex profiles, such as apodisation, difficult to achieve. As gratings now become more sophisticated within the new sensing environment, standard weak gratings used for simple distributed reflection systems are increasingly insufficient. For those applications operating well below the extremes of regeneration, is it possible to retain the advantages of type I gratings? Is there a genuinely distinct threshold between the two? To address these sorts of questions, thermal stabilisation of ordinary type I gratings is revisited with some new ideas based on the description of relaxation and as well on the role of hydrogen in glass. In doing so, we predict and demonstrate, through isochronal annealing, thermal stabilisation of type I gratings to temperatures as high as 600°C simply by annealing at increasing temperatures. In fact, evidence that the thermal stabilisation can be tuned to suit the ideal grating strengths required is presented. A specific aim is for good performance at 400°C, as demanded by many of the industries mentioned earlier. Strikingly, in this work, type I gratings written with pulsed 193nm are characterised with a regeneration threshold temperature of 800°C, about 100°C lower than that obtained using CW 244nm gratings.

### 2.2 Method of thermal stabilisation

Four Bragg gratings (I-IV, L = 10mm) were inscribed into a $H_2$ doped conventional photosensitive germanium and boron co-doped (~33 mol % Ge; ~10mol % B) step index fibre using the 193nm output from an ArF laser. The energy used was well below the damage threshold ensuring gradual positive index growth and normal type I grating behaviour. No rollover in growth was observed ruling out any type 1*n* contributions. The typical grating strengths were ~65 dB, (inset in Fig. 1, shows a typical grating spectra prior

to thermal treatment). For a uniform grating, numerical simulation indicates an index modulation of $\Delta n_{mod} \sim 1 \times 10^{-3}$ so these are strong gratings.

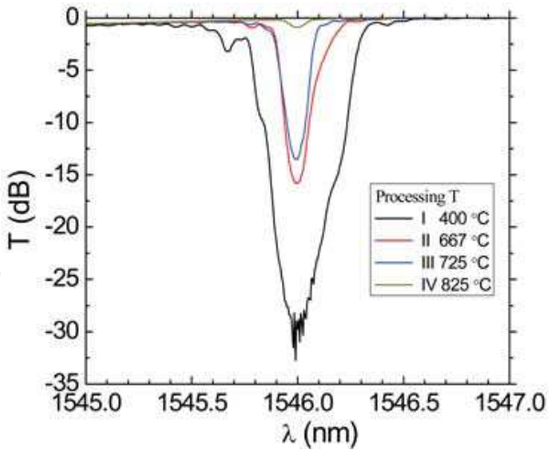


Fig. 1. Transmission spectra of fibre Bragg gratings I-IV with different thermal processing history prior to isochronal annealing.

These gratings were then individually pre-annealed as follows:

I. Ramped in 5 mins to 400 °C, held for 10 min, then removed from heater
II. Ramped in 15 mins to 667 °C, held for 10 mins, then removed from heater
III. Ramped in 15 mins to 667 °C, held for 10 mins, ramped in 10 mins to 745 °C, held for 10 mins, then removed from heater
IV. Ramped in 15 mins to 667 °C, held for 10 mins, ramped in 10 mins to 745 °C, held for 10 mins, ramped in 10 mins to 825 °C, held for 10 mins, then removed from heater

The pre-annealing sequence recipe is important to achieving this stabilisation and there is room for further optimisation. The final grating spectra for each grating are shown in Fig. 2. The large grating strength reduction observed above 800 °C suggests a threshold effect has been reached. As we shall see, this closely corresponds to the temperature at which structural change begins to take place and regeneration occurs.

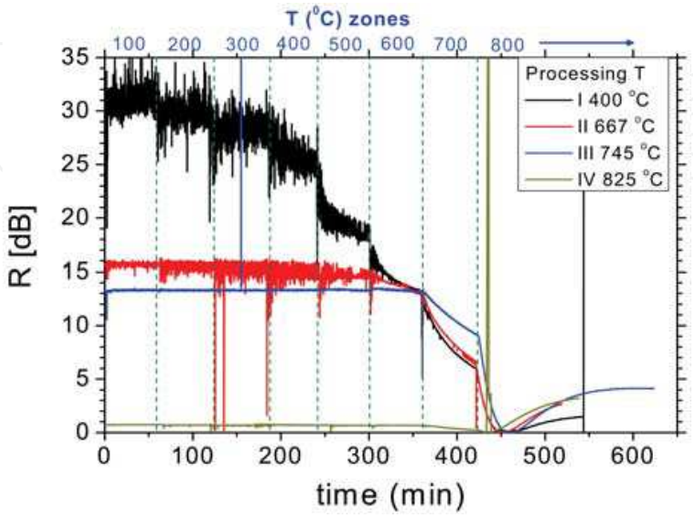


Fig. 2. Isochronal annealing of the four samples as described in the text.

### 2.3 Isochronal annealing

The four gratings were then sequentially isochronally annealed in a high temperature oven in steps of 100 °C for 1hr. A Gaussian fit to the transmission spectra was used to track the grating strength as a function of time (shown in Fig 2). The origin of the observed noise has not been identified but seems to be highest for gratings stronger than 90%. The following observations for each sample are made:

I. No stabilisation as a function of temperature is observed with rapid step decay between temperatures. Partial stabilisation at low temperatures is observed. This behaviour is not dissimilar to that observed for the hypersensitisation of gratings at lower temperatures - 400 °C is higher than the temperature required to form Ge-OH (>300 °C) but lower than that required to form Si-OH (>500 °C) [Sørenson et al. 2005]. Whilst there is some growth and decay observed at lower temperatures, clear exponential decay is observed at 400 °C and beyond.
II. Stabilisation up to and including 500 °C is observed. This is consistent with Si-OH formation and hypersensitisation to these temperatures as previously reported [Sørenson et al. 2005]. At 600 °C and beyond exponential decay is observed.
III. Stabilisation is observed up to and including 600 °C. At 700 °C and beyond exponential decay is observed. Pre-annealing to the higher temperature suggests significant improvement in stabilisation versus only a 2-3dB reduction in grating strength.
IV. The behaviour here is only slightly improved over that of III, suggesting an optimal was being approached with III. It comes at the expense of a very large grating strength reduction (>10dB) suggesting a threshold limit has been exceeded.

From the above results it is clear there is a large scope to adjust the pre-annealing conditions to optimise the thermal stability with the grating strength as required for a specific application. This means there is significant scope for fine tuning grating writing to enable strong gratings of any type to be produced at temperatures suitable for 400 °C operation, those typically used in the oil, gas (including gas sequestration monitoring) and seismic industries. This tuneability is very reminiscent of the thermal tuning we have demonstrated previously for the generation of OH-style gratings using thermal hypersensitisation [Sørenson et al. 2005]. However, it is important to note that if the amorphous nature of the glassy network characterises these processes, similar processes should be possible in glass without hydrogen and, in many cases, irrespective of the processing conditions (including femtosecond induced changes).

An important observation is the reduced threshold for regeneration. In these experiments there is evidence of a threshold-like effect above which regeneration occurs. This seems to be ~800 °C for pulsed 193nm which is at least 100 °C less than that reported earlier for CW 244nm. Further, there is a time dependence for the onset of this regeneration at 800 °C which we believe is probably fibre strain dependent. It also suggests there remains scope for reducing this threshold still further – this is consistent with the changes in local pressure affected by changes in applied strain along the fibre (through Poisson's ratio).

Another striking feature of the thermal stabilisation process is the subsequent single exponential decay readily fitted to the isochronal annealing of the stabilised gratings. Again, the similarities with previous thermal hypersensitisation work are noted [Sørenson et al. 2005; Canning & Hu 2001]. This suggests a single relaxation process is invoked, which is not usual for an amorphous network which is typically is characterised by a distribution of spectral and temporal relaxations that can all be described by single exponentials, though

not all necessarily unique (the general idea of a distribution of Debye relaxations extends to all forms of physical relaxation of viscoelastic solids – see Gross 1968). Generally, the relaxation process is summarised as:

$$N(t) = N_0 \exp[-(t/\tau)^{\beta}] \tag{2.3.2}$$

Where $N$ is the parameter being measured, $N_0$ is the initial value, $t$ is the time, and $1/\tau$ is the rate of relaxation; $\beta$ determines the distribution of relaxation times. In strong glass formers such as silica, $\beta$ is found to be temperature independent and ~0.3 or so. When $\beta = 1$ there is no distribution but a single Debye relaxation. Figure 3 shows the annealing decay profile at 700°C of the grating stabilised at 745°C. A single exponential fits this data. What is unusual is that disordered materials have $\beta < 1$; the implication is that the glass has become far more ordered, perhaps crystalline. If we assume phase separated glass, with the change is confined only to that of silica, an examination of the phase diagram for silica would suggest $\alpha$-quartz, or an analogue, as the likely candidate for a crystalline polymorph. This is an extremely interesting prospect because $\alpha$-quartz is a known piezoelectric material, raising the possibility of all-fibre piezo-based optical devices where the material is introduced periodically or with any profile.

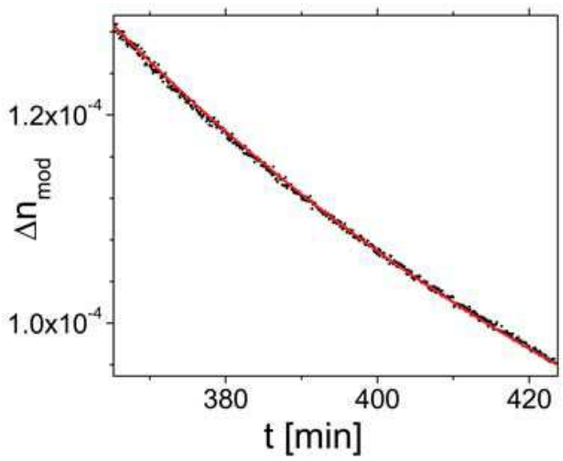


Fig. 3. Decay at 700°C of grating stabilised at 745°C. Single exponential fit also shown.

An approximation of the expected lifetime of a material is often extrapolated from an Arrhenius fit of the rate constant $k = 1/\tau$ where $k = A\exp(-E_a/RT)$. Using similar parameters to those applied in previous work (Inglis 1997; Baker et al. 1997), an estimate of the 3dB lifetime at each temperature for a grating stabilised at 745°C can be obtained, as shown in Figure 4. Although the lifetime falls of rapidly with temperature, these are extremely remarkable results – a grating operating continuously at 400°C can be expected to last for ~10 years, whilst at 350°C >500 years and at 300°C >300,000 years. Further, there remains scope to continue optimising this process.

In conclusion, for many applications, conventional fibre Bragg gratings can be thermally stabilised to operate at temperatures in excess of that required for telecommunications, all the way to 600°C. Beyond this point, regeneration occurs and in this work where pulsed 193nm was used to write the gratings, appears to be characterised by a distinct threshold at 800°C. In contrast, when using CW 244nm light, the threshold seems to be >900°C,

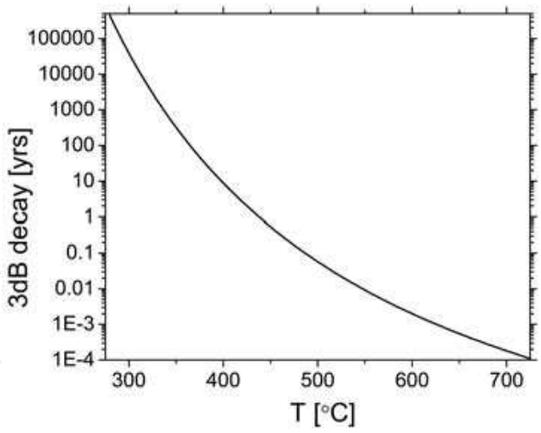


Fig. 4. Lifetime prediction based on 50% (3dB) decay of grating stabilised at 745°C.

suggesting an intensity dependence, and related to this a penetration depth, if the same excitation pathway is assumed. The tuneability offered by thermolytically adjusting, through annealing, the various relaxation processes means its possible to fabricate application specific gratings that require moderate thermal operation to this temperature whilst retaining strong, and sometimes complex (e.g. apodised) reflection spectra, generally not possible by other means. This overcomes one of the current problems associated with weak gratings strengths through regeneration. The versatility of this approach is consistent with the description earlier of an intrinsic distribution of stability regimes and relaxation kinetics that exist within a complex polyamorphous system such as silica. The complex distribution of results accessible by adjusting various parameters from temperature to laser intensity along with temporal processing sheds new insight into annealing generally and more specifically raises interesting questions about the meaning of accelerated ageing tests. This work sets the scene for a more careful evaluation of the processes after which stretched exponential decays reflecting dispersive relaxations, appear less meaningful - above threshold or the onset of regeneration, potentially the onset of crystallisation or a polymorphic (polyamorphic) transition.

## 3. Regeneration

Glass is generally considered to be metastable material with a large distribution of relaxation processes spread in time. As described above, the majority of these relaxations can each be described with a distribution of exponential decays, or Debye relaxations, in dielectric media – therefore, it is not uncommon that the spread of these processes within a random network is described by a stretched exponential distribution governed mostly by one parameter, β [Angell 1995a; Inglis 1997]. It also implies that the thermal processing history and the quenching rate can play a critical role in determining the final index change of the glass. Stretched exponential fits have been successfully used, for example, to determine the aging process of UV-induced periodic changes in glass that make up a fibre Bragg grating [Baker et al. 1997; Inglis 1997]. However, the success of this approach belies the fact that a comprehensive understanding of glass and glassy materials, as a result of the huge distribution of processes in materials that are not governed by an overwhelming and simple periodicity, remains one of the greatest challenges in condensed matter physics. From a practical perspective, for example, although polymorphism of the glassy state

[Mishima et al. 1984, 1985] (or polyamorphism [Wolf et al. 1992, Angell 1995b]) is generally accepted, its role in determining glass structure is rarely invoked when analyzing both thermal and glass transformation for actual device engineering. In photonics, for example, when laser processing is involved, there remains an almost exclusive preference to interpret refractive index changes to defect, or atomic, diffusion as well as direct polarisability changes from localised defect creation or annihilation. On the other hand, as we suggested above the possibility of creating functional polymorphs, such as a-quartz, exists. This introduces the general proposition of how to induce such polymorphic transitions within glass and within an optical waveguide, in this case fibre.

The original premise for our approach to developing high temperature gratings was based on recognizing that the conditions for potentially achieving a pressure-induced transformation of glass, not dissimilar to that reported for ice by Mishima et al. [1994,1995] is seemingly present within an ordinary optical fibre. Optical fibre drawing generally leads to a core glass (often with some germanate to raise the index above the core) which is under tension upon quenching since its thermal expansion coefficient is higher than that of the surrounding glass, which tends to cool first. However, if drawn under appropriate conditions which exploit Poisson's ratio and the fact that vitreous silica tends to have a molar volume larger in the solid state than the liquid state, it is possible to achieve compressive stress. In most typical drawing conditions it is tensile with effective internal pressures that can range from a few tens of MpA to those that exceed 100MpA. These effective internal pressures should allow for an ability to select from within a range of silicate based polyamorphs of varying density and refractive index – (we are not aware of a detailed investigation on this topic as yet). Nonetheless, the fact is that the pre-existing pressures within an optical fibre at the core/cladding interface can be very large and should play a role in a number of phenomena, including photosensitivity and glass. It is almost certain that the rollover from type I gratings to type In (or type IIa) is explained by this as is the observation of a tunable rollover threshold based on longitudinally applied strain (for a review see Canning 2008a).

The only missing ingredient from a post-induced regenerative phase transformation is temperature. If the phase diagram of silica is considered, for a pressure of ~100Mpa and a temperature of 900°C, tridymite (thought to be metastable), and β –quartz are stable. At temperatures above 1470°C, cristabolite is stable – below this it is unstable. Therefore, a simple interpretation of what might occur with thermal processing is that metastable tridymite is formed (perhaps cristabolite at higher temperatures) which the converts to α–quartz upon cooling back to room temperature, since this is the only crystal state stable at ~100Mpa and 25°C. At lower temperatures, as suggested earlier, α–quartz or an analogue involving dopants is feasible and can account for the stabilisation of type I gratings to temperatures in excess of 700°C. For temperatures above this, the conditions must exist for substantially more stable polymorph, or alternatively, polyamorph. In the regimes we are operating at, it is likely that introduced impurities such as hydrogen, will play an additional role given the local strain produced when OH forms, for example. OH formation can lead to stress relaxation in the core and therefore a small structural density change.

The question is how to measure such a transformation – the simplest approach we have is to use a periodically stressed structure which can be characterised optically. A fibre Bragg grating, as we have described, is such a structure. The induced periodic stress of a fibre Bragg grating inscribed with great precision using UV lasers has a modulation close to that

required for our thought experiment to be implemented – a periodic modulation ~50Mpa has been measured in a grating without hydrogen with a spatial resolution of 0.3mm [Raine et al. 1999]. Average UV-induced index changes in excess of 100Mpa have also been reported near the core cladding interface [Raine et al. 1999; Belhadj et al. 2008], suggesting that it is indeed possible to achieve a periodic structure that will seed a periodic regeneration of a different density glass or crystal.

If the possibility of continuous polymorph transformation above the regeneration threshold is accepted, then it is most unlikely the annealing of laser induced changes is going to lead to complete recovery of the glass system – that is, we expect some memory of the UV written "seed" grating to be retained (contrary to a single Debye relaxation below threshold), in particular at the core/cladding boundary. In order to maximise the possibility of achieving high temperature regeneration, hydrogen loading is used for three reasons: *(a)* optimise the induced stress differences between processed and unprocessed regions in the Bragg structure since UV-induced OH causes periodic relaxation of the stresses; and *(b)* minimise the refractive index contribution of the UV written grating to the polarisability changes associated with OH formation; and *(c)* reduce the chance of eventually relaxing to crystallised $\alpha$ quartz which has the potential of changing to other structures each time the grating is heated to higher temperatures (this can explain why the results of Linder et al. 2009, and indeed most type I*n* (type IIa), are unstable above 600°C).

Therefore, the experiment is to write a standard grating in photosensitive fibre loaded with hydrogen and post-anneal this gradually to 900°C and beyond. If this model is correct, then it should be possible to thermally process a fibre and transform the grating from an ordinary type I grating, for example, to an ultra-stable regenerated grating far exceeding the properties of the thermally stabilised gratings described in the previous section. To maximise the chance of the process working, the original experiments focused on strong fibre Bragg gratings written with hydrogen. The results reported in [Canning et al. 2008b] verify that a new grating structure which was stable up to 1295°C before the fibre broke could be obtained. Despite the deterioration and breaking of the fibre in an open environment at such temperatures, the remaining regenerated grating remained intact when broken pieces were analysed, consistent with a stronger glass than the original glass. The nature of this glass is not yet resolved but preliminary scanning electron microscopy (SEM) analysis suggests a reduced Si concentration within the fibre. Figure 5 shows the results – no change in Ge concentration is revealed, pointing towards a transformation of silica and not germanosilicate. The results are also hinting that that change is indeed located more at the interface – however, more comprehensive work is necessary to understand these results further. Indirect support for the results appears when a detailed study of the role of germanium is investigated – despite varying the concentration of $GeO_2$ from ~3mol% (standard telecommunications fibre) to >20mol%, for equal seed grating strengths, the regenerated grating of similar strength is obtained. This suggests strongly that the regeneration is largely independent of the germanium concentration – it is not obvious how this fits into a general distribution of relaxations in an amorphous network but germanium dioxide, whilst having many structural analogies to silicon dioxide, has significant thermal history differences because of weaker bonding and a much lower melting point (~1100°C).

The likelihood of a more complex polyamorphic transition spectrum is increased when conditions for the threshold transformation are shown to be sensitive to a number of parameters, including writing intensity: using CW 244nm written gratings in standard

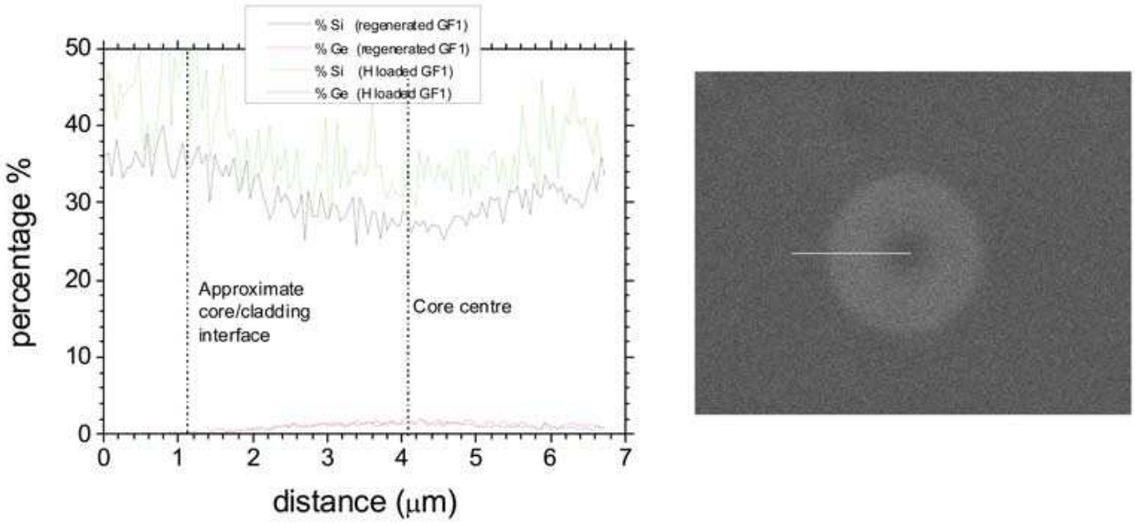


Fig. 5. X-ray backscatter analysis of germanosilicate core fibre with hydrogen loading and no grating, and another identical fibre containing a regenerated grating. No change in Ge concentration is observed whilst there is ~10% reduction in Si, consistent with a density drop in the silica (Preliminary data collected by Matthew Kolibac, 2009, Electron Microscope Unit, University of Sydney).

photosensitive fibre requires ~900°C to be reached, whilst for gratings written with 193nm pulsed light it appears that temperature can be reduced to 800°C [Åslund et al. 2009a; Canning et al. 2009]. More interestingly, perhaps, below the regeneration "threshold", the annealing phenomena we have observed is much closer to the idealised spectrum of polymorphic transformation: we have proposed and demonstrated "tuning" of the thermal stability of fibre Bragg gratings so that they can be tailored to operate at arbitrary temperatures, well in excess of type I gratings but below that of regenerated gratings [Åslund et al. 2009a; Canning et al. 2009].

Here, we focus on regenerated gratings within hydrogen loaded standard photosensitive optical fibres since this gives the most pronounced stabilisation to date. Since our work, others [Linder et al. 2009] have shown that regeneration can be obtained at lower temperatures in gratings written without hydrogen – the low thermal stability of these gratings is consistent with type 1*n* gratings. If crystallisation is occurring it is likely to be via the mechanism we described above to $\alpha$–quartz, which is stable at ~100Mpa close to the observed 600°C. Whatever the state of glass, it is clearly distinct from that obtained at higher temperatures with hydrogen – if the general model described earlier holds, it is possible that at higher temperatures, a secondary regeneration process is observed in fibres without hydrogen (since it is not essential to the basic tenet). Interestingly, it appears that the procedures involved with thermal stabilisation may be important to achieving the subsequent regeneration – straight heating up to the regeneration temperature produced very poor results and in many instance none at all. This may indicate that the initial structural change which occurs is important to the subsequent regeneration process.

In the following sections, we describe how regenerated gratings are fabricated and characterise their annealing behaviour. An important practical consideration is the quality and resolution achievable with these gratings. We explore this by examining the regeneration of much more complex structures than simple uniform gratings.

### 3.1 Fabrication of seed gratings

In order to precipitate the structural change associated with regenerated gratings, a seed grating is necessary. In practice, we have confirmed that the stronger the seed grating, the stronger the final regenerated grating. For this case, a conventional Bragg grating inscribed into hydrogen loaded (24hrs, 200atm, 70°C) relatively highly germanium doped step index fibre with no boron ($r_{core}$ ~ 2μm, [$GeO_2$ ~ 10.5mol%], $\Delta n_{co/cl}$ = 0.012), using the 244nm output from a frequency doubled $Ar^+$ laser (P ~ 50W/cm², $f_{cumulative}$ ~ (6-12)kJ/cm², the same as that reported in Bandyopadhyay et al. 2008 and Canning et al. 2008b). Figure 6 shows the transmission and reflection of a very strong type I Bragg grating, readily exceeding the noise floor in transmission of our tunable laser and power meter setup (res: 1pm). Ignoring the slight quadratic chirp in the transmission profile, the simulation spectra for a uniform grating, based on transfer matrix solution of the coupled mode equations, was fitted to the bandwidth to estimate the index modulation achieved: $\Delta n_{mod}$ ~ 1.6 x $10^{-3}$, consistent with a grating >120dB in strength.

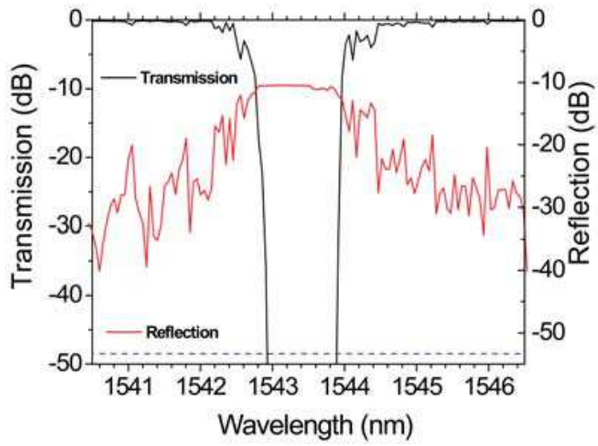


Fig. 6. Transmission and reflection spectra of the "conventional" seed grating. Noticeably, the large side lobes of this structure obscure the stitching errors expected from the phase mask used. The dashed line represents the noise floor.

### 3.2 Fabrication of regenerated gratings

Using a processing procedure identical to that optimised in Bandyopadhyay et al. 2008 and Canning et al. 2008b, ultra strong seed gratings were thermally processed sequentially with a standard recipe. At 950°C the onset of regeneration is observed, and over time as the seed grating disappears completely, the regenerated grating appears. The final transmission and reflection spectra of the regenerated grating, obtained from the seed grating shown in figure 6, are shown in figure 7. It is more than 50dB in strength and below the noise floor. Numerical simulation indicates an index modulation of $\Delta n_{mod}$ ~ 1.55 x $10^{-4}$, which is substantial. However, the average index may likely be greater than this since the Bragg wavelength, $\lambda_B$, tends to be shifted to longer wavelengths to that of the seed grating at room temperature, indicating that the fringe contrast is not optimal, potential scope for improvement.

In order to study the growth and annealing properties, a second regenerated grating was made from a weaker seed grating, written with a cumulative fluence ~30% less than that of the first grating, so that the full transmission spectrum can be observed within the noise

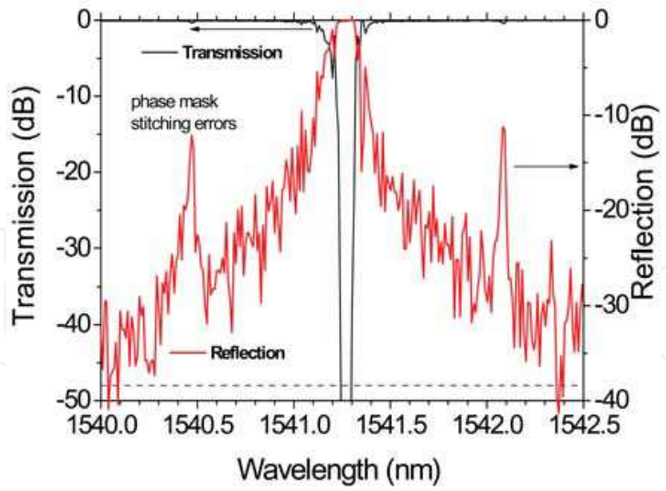


Fig. 7. Transmission and reflection spectra of the regenerated grating. Noticeably, the stitching errors of the phase mask are clearly visible indicating all the relative phase information has been retained. The dashed line represents the noise floor.

floor of the tunable laser and power meter setup. Figure 8 shows a close-up of the grating formation over time at ~950˚C – in this example, the structure is less uniform with a quadratic chirp present. This chirp is an exaggerated copy of the seed grating quadratic chirp so the complex profile of the seed grating was preserved. When tension is removed during regeneration, $\lambda_B$ is the same between seed and regenerated grating, also consistent with our previously reported observations [Bandyopadhyay et al. 2008; Canning et al. 2008b].

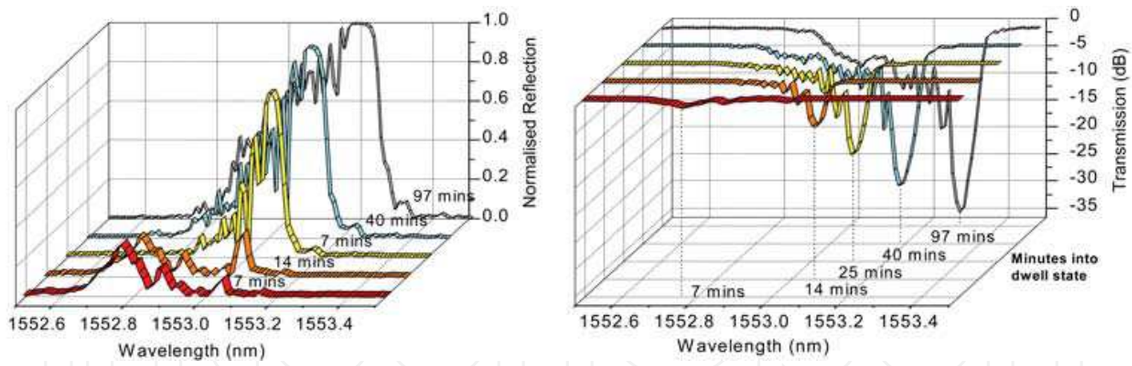


Fig. 8. Reflection (normalised) and transmission spectra during formation and growth of regenerated grating. Significant, amplified quadratic chirp is observed.

## 4. Annealing

The regenerated grating, shown in figure 7, was then cycled back to room temperature, back up to 1100˚C and back to room temperature. For the short exposure times of ~10mins at each temperature every 100˚C, no changes are observed in the grating spectra within the noise floor. The second regenerated grating was used to determine the longer term performance at 1000˚C and 1100˚C. The regenerated grating, ~42dB in strength, was cooled back to ~200˚C before being taken up to 1000˚C to show that no decay occurs at lower temperatures. The

grating was then ramped to 1100˚C over ~50 minutes. It was then allowed to sit at 1100˚C for an additional 4 hours and 10 minutes. During the ramping period the grating decays with a single exponential to ~19dB. This stabilised to a final rejection of ~18dB within ten minutes at 1100˚C. The grating strength after this point remained constant over the remaining exposure period. Figure 9 (a) shows a full summary of seed grating decay, regeneration formation and then the annealing results whilst figure 9 (b) shows a contour image diagram of the decay process over time showing the Bragg wavelength shift with temperature, the exponential decay in contour form and the subsequent stable and steady performance after an hour.

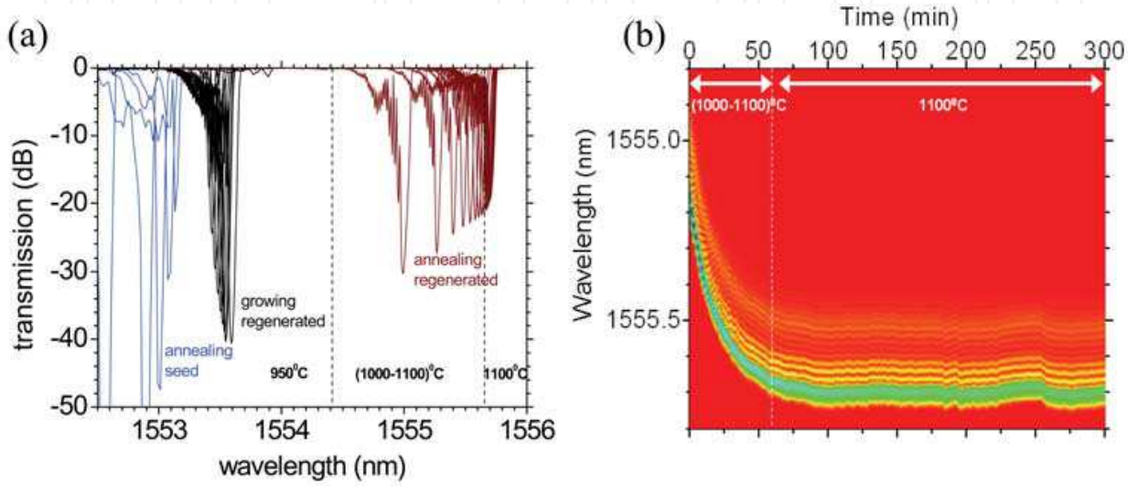


Fig. 9. (a) Summary of seed grating decay, regenerated grating formation and annealing; (b) detailed examination of the annealing of the grating between 1000 and 1100 ˚C.

When comparing with our previous work, we have shown that by simply extending the length of the seed grating we can regenerate longer gratings that increased in strength approximately linearly after stabilisation. In the previous work, the regenerated grating was reported to be ~2.3dB over 0.5cm, or a coefficient of 4.6dB/cm within the same fibre used here and for the same seed grating writing conditions. The reported value for 5cm in this work after stabilisation is ~18dB, less than the 23dB expected – this is because the seed grating fluence of this grating was actually less than that used previously so as to be able to observe the peak regeneration, ~42dB, prior to stabilisation. (The first grating broke during experiments so additional stabilisation could not be pursued). Within experimental error, there is no evidence to suggest a non-linear regenerated grating strength with length in this fibre.

The observation that the regenerated grating is stabilised after an initial decay process suggests two contributions to the grating strength, the second contribution clearly enabling extremely strong thermal resistance of the grating (up to 1295˚C as demonstrated in Canning et al. 2008b). The single exponential process supports the notion that the first decay process is indeed a singular one. It too is quite stable after formation at least at temperatures below the regeneration temperature of ~950˚C. Given the localisation of the changes to the periodic scale of the seed grating, the likely contributions are related to stresses not only at the core-cladding interface but indeed between processed regions. What is important to note is that the decrease in grating strength does not appear to be accompanied by any average index decrease (i.e. $\lambda_B$ continues to be red-shifted and no blue shift is observed though its difficult

to separate this because of the slow thermal equilibration of the oven used). Based on this observation, the appearance of two contributions may be an artifact of gradual fringe relaxation until the one contribution is stabilised – this suggests there is a longitudinal component (through stress between processed and unprocessed regions).

### 4.1 Dependence on germanium dioxide concentration [$GeO_2$]

With regards to the mechanism of formation, we have ruled out the role of fluorine in the cladding in this process by observing nearly identical regeneration (actually slightly reduced) and annealing within fibres that have no fluorine at all. The SEM observation in figure 5 reveals an apparent reduction in [Si] after regeneration, consistent with a decrease in silica density (and therefore oxygen as well). In contrast, no change in Ge concentration is observed. This suggests that the concentration of $GeO_2$ is not a direct factor in regeneration. To explore this, gratings were written in fibres with varying concentration, from ~3 mol% used in standard telecommunications grade optical fibre to ~30 mol% in highly photosensitive fibres. In all these cases, for gratings with the same seed index modulation (strength), the regenerated gratings are identical in strength. What is important is the initial seed grating strength and not [$GeO_2$]. This supports the null result from the SEM data.
The regenerated grating strength obtained is shown to be determined by a number of factors including seed grating strength and as well the fibre V parameter determined from both numerical aperture (NA) and core radius. More complex results appear to be obtained when additional dopants are employed. Early results indicate that when a fibre has 3 times the concentration of $GeO_2$ than the fibre used here, but is loaded with $B_2O_3$ to reduce the numerical aperture and allow a larger core radius, we find the regenerated grating strength is less than half. $B_2O_3$ is also a glass softener and can significantly change the internal frozen-in stresses of the fibre during drawing. This supports the idea that stress is important in the regeneration process (and indeed below it). More detailed scientific studies are currently underway to explore the changes involves.

## 5. Regeneration of complex gratings

In order to determine whether this process can be applied beyond simple Bragg grating writing as a realistic approach to the production of complex gratings and patterns and structures that can operate at high temperature whilst retaining the complexity of a nano-scaled device, we explored the impact of the regeneration process on two complex grating structures: (1) structure consisting of two superposed gratings with $\lambda_1 \sim 1548.73$ nm and $\lambda_2 \sim 1553.56$ nm, i.e. with $\Delta\lambda \sim 4.8$nm; and (2) a dual channel grating produced by writing a Moiré grating. In a Moiré grating, the refractive index variation along the length of the grating is also different where a uniform period, $\Lambda_B$, is modulated by a low spatial frequency sinusoidal envelope of period, $\Lambda_e$, that produce two sidebands (essentially a phase shifted structure built up from a periodic distribution of identical phase shifts). Given the sensitivity of the Moire grating to any perturbation in phase, the preservation of the transmission notch and overall profile will be indicative of nanoscale resolution in the regenerated structure.
For the superposed gratings (L ~ 5 mm) were inscribed into a $H_2$ loaded (24hrs, P = 100atm, T = 100˚C) $GeO_2$ doped core silica fibre ([$GeO_2$] ~ 10%, fabricated at CGCRI) using a pulsed KrF exciplex laser (248 nm, pulse duration = 20 ns, $f_{\text{pulse}} \sim 70$ mJ/cm², repetition rate = 200

Hz). The Moiré grating was written into a fibre which was similar to that used for the superposed grating but also had boron to increase the seed photosensitivity. Regeneration is carried out with an identical recipe to that described earlier but inside a short fibre micro-heater. The hot zone of this heater is supposedly uniform over 5mm only (the exact variation along this length is not known but we suspect a Gaussian profile), and this dictates the grating length.

### 5.1 Superposed gratings

Sample #1 was prepared by superposing two seed gratings with Bragg wavelengths $\lambda_1$ ~ 1548.73 nm and $\lambda_2$ ~ 1553.56 nm, i.e. with $\Delta\lambda$ ~ 4.8nm. Each of the seed gratings was of moderate strength with transmission loss at $\lambda$ ~ -20 dB (grating with $\lambda_1$ being slightly stronger than that at $\lambda_2$). The superposition of two gratings leads to a compound form of the local index modulation described as [Bao et al. 2001]:

$$\Delta n(z) = 2\Delta n_0 Cos\left(\frac{\pi(2\Lambda_{B1}+\Delta\Lambda)}{\Lambda_{B1}(\Lambda_{B1}+\Delta\Lambda)}z+\frac{\Delta\Phi}{2}\right)Cos\left(\frac{\pi\Delta\Lambda z}{\Lambda^2}-\frac{\Delta\Phi}{2}\right) \quad (1)$$

$\Lambda_{B1}$ and $\Lambda_{B2}$ are the periods of the gratings with $\Lambda_{B2} = \Lambda_{B1}+\Delta\Lambda$ and $\Delta\Phi$ is the initial phase difference of the gratings. It is clear from this expression any non-uniformity introduced by the thermal annealing process will result in a spread of $\Delta\Phi$ and broadening of the peaks. The structure was then thermally processed as described earlier until regeneration was complete. The results are summarised in figure 10. Within experimental uncertainty, the Bragg wavelength separation remains the same (~4.8nm) although, as expected the annealing has led to a decrease in average index so that the Bragg wavelengths are blue-shifted. This reduction leads to a change in the phase distribution and the regenerated gratings have a more asymmetric profile, shown in the inset of figure 10 (c). This is consistent with a very weak Gaussian, or quadratic, chirp on the grating. The origin for this chirp almost certainly arises from the hot zone temperature distribution of the micro-heater rather than any intrinsic grating property.

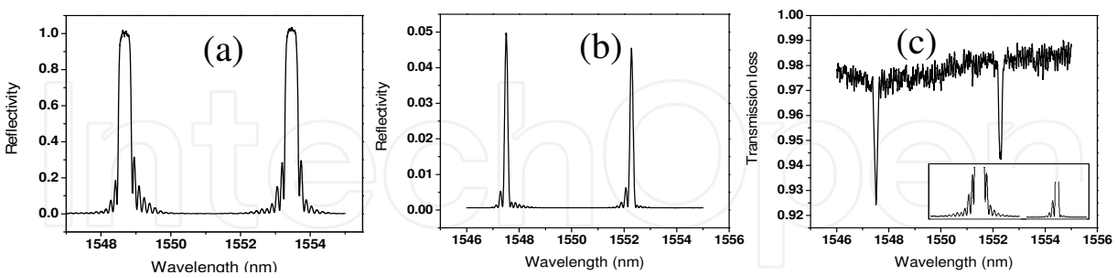


Fig. 10. Spectrum of dual over-written gratings. (a) Normalised reflection spectrum of the seed; (b) and (c) reflection and transmission spectrum of the regenerated grating respectively represented in absolute scale. Inset: close-up of side lobe structure of right hand peaks of seed and regenerated grating for comparison.

### 5.2 Moiré gratings

In a Moiré grating, a uniform period, $\Lambda_B$, is modulated by a low spatial frequency sinusoidal envelope of period, $\Lambda_e$, (figure 11) that produces two sidebands. The structure is equivalent to two gratings with stopgaps that overlap sufficiently to produce a resonant phase shift–

like structure in the stop gap of the superstructure. A similar profile is obtained by placing phase shifts with a low frequency period along a uniform grating.

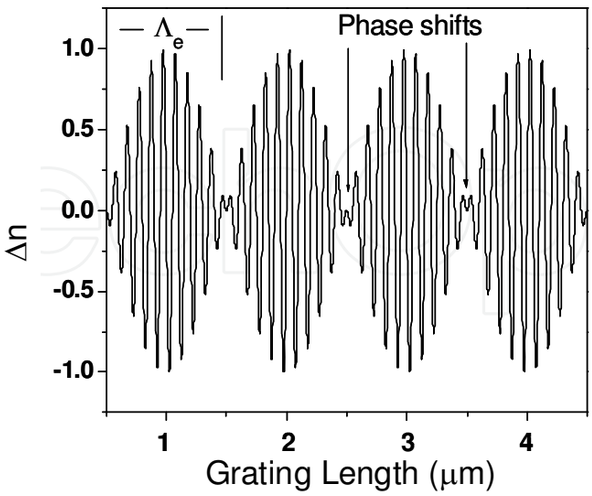


Fig. 11. Index modulation introduced into the seed Moiré grating.

The position dependent index amplitude modulation profile can be described as [Ibsen et al. 1998]:

$$\Delta n(z) = 2n\Delta n_0 F(z) Cos\left(\frac{2\pi Nz}{\Lambda_B}\right) Cos\left(\frac{2\pi Mz}{\Lambda_e}\right) \tag{2}$$

where $N$ and $M$ are integer and $2n\Delta n_0$ is the UV induced index change, $F(z)$ is the apodisation profile. On simplifying, eq.(2) directly leads to the resultant spatial frequencies at the sum and difference frequencies where two Bragg reflections will occur and may be represented as:

$$\Delta n(z) = n\Delta n_0 F(z)\left\{\cos\left(\frac{2\pi N}{\Lambda_B}\left[1+\frac{M\Lambda_B}{N\Lambda_e}\right]z\right)+\cos\left(\frac{2\pi N}{\Lambda_B}\left[1-\frac{M\Lambda_B}{N\Lambda_e}\right]z\right)\right\} \tag{3}$$

The new reflection has two effective bands separated in wavelength, $\Delta\lambda$, as:

$$\Delta\lambda = \frac{{\lambda_B}^2}{2n_{eff}\Lambda_e} \tag{4}$$

Based on the principle mentioned above a dual seed grating with a 100 GHz separation i.e. $\Delta\lambda \sim 0.8$ nm was written. Selected $\Lambda_B$ = 533.17 nm produces a grating with $\lambda_B \sim 1554$ nm. Modulating $\Lambda_B$ with $\Lambda_e$ = 1028 μm we could generate two channels Bragg wavelengths, $\lambda_1$ = 1553.51nm and $\lambda_2$ = 1554.34 nm respectively. The effective refractive index of the fibre is $n_{eff}$ = 1.4573. A precisely controlled scanning beam writing setup was used to produce $\pi$-phase shifts at specific locations of the grating to generate the required low frequency sinusoidal modulation of the index profile. A summary of the induced profile is shown in figure 6. The seed grating reflection profile is shown in figure 12 (a) and the regenerated grating reflection and transmission profiles are shown in figures 12 (b) & (c). Unlike the superposed gratings,

where the sidebands of the grating are a result of the interference between end reflections of the grating and therefore susceptible to temperature gradients in the micro heater hot zone, the interference in the phase shift region is a result of the distributed interference between the grating and super period of the phase shifts. This means the structure is less sensitive to overall gradients on a macro scale. Importantly, the interference in the phase shift region is preserved after regeneration indicating that despite the very large macro heating process involved in creating the regenerated grating, the structure retains full memory of the seed grating, indicating that there is no evidence of a diffusive process that would alter the phase relationship anywhere over the grating length. Full preservation on a nanoscale is maintained through regeneration – this is a remarkable result.

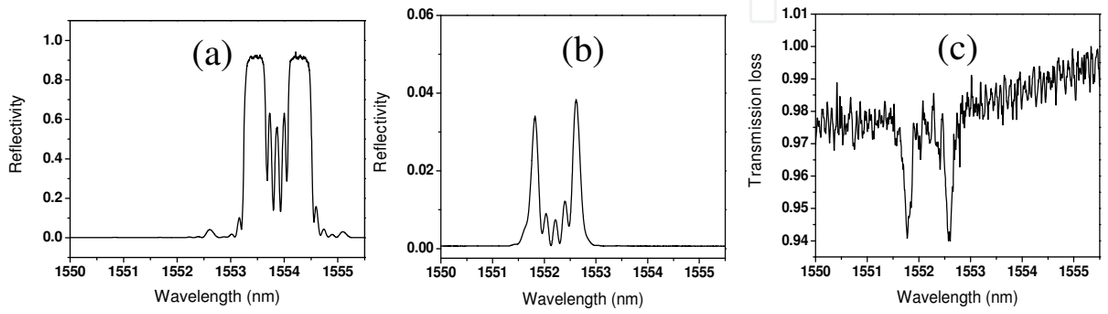


Fig. 12. Spectrum of Moiré grating. (a) Normalised reflection spectrum of the seed, (b) and (c) reflection and transmission spectrum of the regenerated grating respectively represented in absolute scale.

## 6. Conclusion

Strong regenerated gratings (~18dB, L = 5cm) that can withstand temperatures in excess of 1200°C have been produced. These gratings have a number of potential applications from monitoring furnace temperatures in various fields, to high intensity optical field-resistant gratings for high peak power fibre lasers. Below the regeneration threshold, stabilisation of type I gratings offers a realistic prospect of balancing grating strength with practical temperature operation up to 700°C. Remarkably, single exponential relaxation, consistent with annealing of a regular rather than an amorphous structure, is observed during isochronal annealing of thermally stabilised type I gratings.

Retaining the complex functionality available to type I gratings has also been demonstrated. In particular, complex regenerated gratings (L = 0.5cm) were produced. Two dual channel filter designs – a superposed grating and a Moiré grating – were fabricated with more than 4% transmission. The regenerated superposed structure showed signs of a small chirp possibly arising from the slightly Gaussian profile of the micro heater hot zone employed. This suggests that regenerated gratings can be thermally post-tailored during regeneration from the seed grating on a macro scale. In contrast, despite the significantly reduced strength and the reduced average index change (measured as a shift to shorter wavelengths) the regenerated Moiré grating exactly preserved the interference profile within the central transmission notch of the grating spectrum, and therefore the embedded phase information of the seed grating.

Preliminary material analysis using SEM backscattered x-rays and comparing results between fibres of different compositions indicates an independence of $GeO_2$ concentration. The SEM results suggest there is a reduction of Si and no reduction of Ge, consistent with a stress (pressure) driven silica transformation. This drop in Si is across the core though the changes, experimental variation not withstanding, appear higher at the core/cladding interface – periodic longitudinal stress profiles between processed regions within the seed grating maybe equally important to any interface effects. The regenerated grating strength appears to be mainly dependent on the initial seed grating modulation, or grating strength. This is also consistent with the extraordinary localisation of the thermally induced change with the original seed grating.

Given that much of the general process involves glass re-quenching under a different thermal history, both the thermal stabilisation and the regenerative processes described here are unlikely to be confined to silica fibres loaded with or without hydrogen (as recent results indicate). Rather, both processes have huge scope to be applied to many numerous materials systems – for example, stresses (and therefore equivalent pressures) at interfaces can be controlled by many means including the use of different thin film layers [Canning 2001]. It opens the way of using nanoscale precision laser processing to introduce nanoscale patterns and structures in materials which can then be thermally processed, with unique recipes given each environment, for additional stability. We believe regeneration has the potential to greatly expand advanced holographic processing of systems and templates by extending the lifetime and operational thresholds of the materials to a level not previously thought possible. This will be particularly important within applications involving very high intensity optical fields such as pulsed lasers.

Finally, the use of an optical fibre grating as the test bed for exploring thermal annealing of glasses generally has been proposed, offering a novel way to study the complex relaxations possible in glasses, including mixed systems.

## 7. Acknowledgements

We would like to acknowledge various colleagues who have helped prepare this work, including Jacob Fenton (a summer student at iPL) and Matthew Kolibac who have worked on various aspects of regenerated gratings. Funding from the Australian Research Council (ARC) and an International Science Linkage Grant from the Department of Industry, Innovation, Science and Research (DIISR), Australia and the Council of Scientific and Industrial Research (CSIR), India, under the 11th five year plan is acknowledged.

## 8. References

Åslund, M. & Canning, J. (2000). "Annealing properties of gratings written into UV-presensitized hydrogen-out diffused optical fiber", *Opt. Lett.* 25, 692-694

Åslund, M.; Jackson, S.D.; Canning, J.; Groothoff, N.; Ashton, B. & Lyytikainen K. (2005). "High power $Yb^{3+}$ doped air-clad fibre laser using a Bragg grating written into the active medium", *Australian Conference on Optics and Lasers and Spectroscopy (ACOLS 2005)*, Roturua, New Zealand, paper WeA2

Åslund, M. L.; Jovanovic, N.; Jackson, S. D.; Canning, J.; Marshall, G. D.; Fuerbach, A. & Withford M. J. (2008). "Photo-annealing of femtosecond laser written Bragg

gratings", *Australian Conference on Optical Fibre Technology & Opto-Electronics and Communications Conference, (ACOFT/OECC 08)*, Darling Harbour, Sydney

Åslund, M. L.; Canning, J.; Stevenson, M. & Cook, K. (2009a). "Thermal stabilisation of type I grating", *IEEE Photonics Society Annual Meeting*, Turkey

Åslund, M. L.; Jovanovic, N.; Canning, J.; Jackson, S. D.; Marshall, G. D.; Fuerbach, A. & Withford M. J. (2009b). "Photo-annealing of femtosecond laser written Bragg gratings", Accepted to *Photonic Technology Letters*

Angell, C. A. (1995a). "Formation of Glasses from Liquids and Biopolymers", *Science* 267, 1924

Angell, C. A. (1995b). "The old problems of glass and the glass transition, and the many new twists", *Proc. Natl. Acad. Sci. USA* 92, 6675-6682

Archambault, J.L.; Reekie L. & Russell, P. St. (1993). "100% reflectivity Bragg reflectors produced in optical fibres by single excimer laser pulses", *Electron. Lett.* 29, 453-455

Baker, S. R.; Rourke, H. N.; Baker, V. & Goodchild, D. (1997). "Thermal decay of fiber Bragg gratings written in boron and germanium codoped silica fiber", J. Lightwave Tech. 15 (8), 1470-1477

Bao, J.; Zhang, X.; Chen, K. & Zhou, W. (2001). "Spectra of dual overwritten Bragg grating", *Optics Commun.* 188, 31-39

Bandyopadhyay, S.; Canning, J.; Stevenson M. & Cook, K. (2008). "Ultrahigh-temperature regenerated gratings in boron-codoped germanosilicate optical fiber using 193 nm", *Opt. Lett.* 33 (16), 1917-1919

Belhadj, N.; Park, Y.; LaRochelle, S.; Dossou, K. & Anzana J. (2008). "UV-induced modifications of stress distribution in optical fibres and its contribution to Bragg grating birefringence", *Opt. Express* 16 (12) 8727-8741

Butov, O.V.; Dianov E. M. & Golant, K.M. (2006). "Nitrogen-doped silica core fibres for Bragg grating sensors operating at elevated temperatures," *Meas. Sci. Technol.* 17, 975-979

Canning, J.; Sommer, K. & Englund, M. (2001). "Fibre gratings for high temperature sensor applications", *Meas. Sci. Tech.* 12, 824-828

Canning, J. (2001)."Birefringence control in planar waveguides using doped top layers", *Opt. Comm*. 191, (3-6), 225-228

Canning, J. & Hu, P-F. (2001). "Low temperature hypersensitisation of phosphosilicate waveguides in hydrogen", *Opt. Lett*., 26 (16), 1230-1232

Canning, J. (2006). Fibre lasers and related technologies, *Opt. & Las. In Eng*., 44, 647-676

Canning, J. (2008a). Fibre Gratings and Devices for Sensors and Lasers, *Lasers and Phot. Rev.* 2 (4), 275-289

Canning, J.; Stevenson, M.; Bandyopadhyay, S. & Cook, K. (2008b). "Extreme Silica Optical Fibre Gratings", *Sensors* 8, 6448-6452

Canning, J.; Åslund, M.; Stevenson, M. & Cook, K. (2009). Australian Conference on Optical Fibre Technology (ACOFT 2009), Adelaide, Australia

Cardozo da Silva, J.C.; Martelli, C.; Kalinowski, H.J.; Penner, E.; Canning J. & Groothoff, N. (2007). "Dynamic analysis and temperature measurements of concrete cantilever beam using fibre Bragg gratings", *Opt. & Las. in Eng.* 45 (1), 88-92

Dong, L.; Liu W.F. & Reekie L. (1996). "Negative index gratings formed by 193nm laser", *Opt. Lett.* 21 (24), 2032-2034

Epaarachchi, J.; Canning, J. & Stevenson M. (2009). "An investigation of response of embedded near infrared fibre Bragg grating (FBG) sensors (830nm) in glass fibre composites under fatigue loading", Accepted to *J. of Composite Materials*
Online at: http://jcm.sagepub.com/cgi/content/abstract/0021998309346382v1

Fokine, M. (2002). "Formation of thermally stable chemical composition gratings in optical fibers", *J. Opt. Soc. Am. B* 19, 1759-1765

Grobnic, D.; Smelser, C.W.; Mihailov, S.J. & Walker, R.B. (2006). "Long term thermal stability tests at $1000^0$C of silica fibre Bragg gratings made with ultrafast laser radiation," *Meas. Sci. Technol.* 17, 1009-1013

Groothoff, N. & Canning, J. (2004). "Enhanced type IIA gratings for high-temperature operation", *Opt. Lett.* 29, 2360-2362

Gross, B. (1968). *Mathematical Structure and Theories of Viscoelasticity*, (Paris: Herman)

Hill, P.; Atkins, G.R.; Canning, J.; Cox, G.; Sceats, M.G. (1995). "Writing and visualisation of low threshold type II Bragg gratings in stressed optical fibres", *Appl. Opt.* 33 (33), 7689-7694

Ibsen, M.; Durkin, M.K. & Laming, R.I. (1998). "Chirped Moiré fiber gratings operating on two wavelength channels for use as dual-channel dispersion compensators," *IEEE Photon. Tech.. Lett.* 10, 84–86

Inglis, H. G. (1997). ''Photo-induced effects in opticals fibres,'' Ph.D. dissertation (School of Chemistry, University of Sydney, Sydney, NSW, Australia, 1997).

Kersey, D. (2000). "Optical fiber sensors for permanent downwell monitoring in the oil and gas industry", *IEICE Trans.* E83-C (3), 400-404

Linder, E.; Chojetski, C.; Brueckner, S.; Becker, M.; Rothhardt, M. & Bartelt, H. (2009) "Thermal regeneration of fibre Bragg gratings in photosensitive fibres", *Opt. Express* 17, 12523-12531

Mishima, O.; Calvert, L. D. & Whalley, E. (1984). " 'Melting ice' I at 77 K and 10 kbar: a new method of making amorphous solids," *Nature (London)* 310, 393-395

Mishima, O.; Calvert, L. D. & Whalley, E. (1985). "An apparently first-order transition between two amorphous phases of ice induced by pressure," *Nature (London)* 314, 76-78

Raine, K.W.; Feced, R.; Kanellopoulos, S.E. & Handerek, V.A. (1999). "Measurement of Axial Stress at High Spatial Resolution in Ultraviolet-Exposed Fibers," *Appl. Opt.* 38, 1086-1095

Schroeder, R.J.; Yamate, T. & Udd, E. (1999). "High pressure and temperature sensing for the oil industry using fibre Bragg ratings written into side hole single mode fibre", *Proc. SPIE* 3746, 42-45

Shen, Y.; He, J.; Qiu, Y.; Zhao, W.; Chen, S.; Sun, T. & Grattan, K.T. (2007). "Thermal decay characteristics of strong fiber Bragg gratings showing high temperature sustainability", *J. Opt. Soc. Am. B* 24, 430-438

Sørenson, H. R.; Canning, J.; Kristensen, M. (2005). "Thermal hypersensitisation and grating evolution in Ge-doped optical fibre", *Opt. Express,* 13 (7), 2276-2281

Trpkovski, S.; Kitcher, D.J.; Baxter, G.W.; Collins, S.F. & Wade, S.A. (2005). "High temperature-resistant chemical composition gratings in $Er^{3+}$-doped optical fiber," *Opt. Lett.* 30, 607-609

Wolf, G. H.; Wang, S.; Herbst, C. A.; Durben, D. J.; Oliver W. J.; Kang, Z. C. & Halvorsen, C. (1992) in *High Pressure Research: Application to Earth and Planetary Sciences*, eds.

Manghnani, Y. S. & Manghnani, M. H. (Terra Scientific/Am. Geophys. Union. Washington, USA), pp.503-517

Xie, W.X.; Niay, P.; Bernage, P.; Douay, M.; Bayon, J.F.; Georges, T.; Monerie, M. & Poumellec, B. (1993). "Experimental evidence of two types of photorefractive effects occurring during photo inscriptions of Bragg gratings within germanosilicate fibers", *Opt. Commun.* 104, 185-195

Zhang, B. & Kahriziet, M. (2007). "High temperature resistance fiber Bragg grating temperature sensor fabrication", *IEEE Sensor J.* 7, 586-590

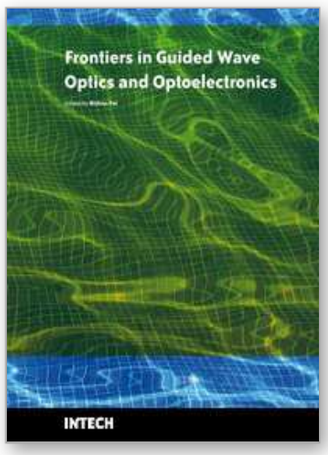


**Frontiers in Guided Wave Optics and Optoelectronics**

Edited by Bishnu Pal

ISBN 978-953-7619-82-4
Hard cover, 674 pages
**Publisher** InTech
**Published online** 01, February, 2010
**Published in print edition** February, 2010

As the editor, I feel extremely happy to present to the readers such a rich collection of chapters authored/co-authored by a large number of experts from around the world covering the broad field of guided wave optics and optoelectronics. Most of the chapters are state-of-the-art on respective topics or areas that are emerging. Several authors narrated technological challenges in a lucid manner, which was possible because of individual expertise of the authors in their own subject specialties. I have no doubt that this book will be useful to graduate students, teachers, researchers, and practicing engineers and technologists and that they would love to have it on their book shelves for ready reference at any time.



INTECH
open science | open minds

**InTech Europe**
University Campus STeP Ri
Slavka Krautzeka 83/A
51000 Rijeka, Croatia
Phone: +385 (51) 770 447
Fax: +385 (51) 686 166
www.intechopen.com

**InTech China**
Unit 405, Office Block, Hotel Equatorial Shanghai
No.65, Yan An Road (West), Shanghai, 200040, China
中国上海市延安西路65号上海国际贵都大饭店办公楼405单元
Phone: +86-21-62489820
Fax: +86-21-62489821

IntechOpen